

SURFACE CONTROL OF ACTUATED HYBRID SPACE MIRRORS

Brij. N. Agrawal

Naval Postgraduate School, Monterey, CA, 93943, agrawal@nps.edu

Jae Jun Kim

Naval Postgraduate School, Monterey, CA, 93943, jki1@nps.edu

This paper presents active surface control techniques for space mirrors. These techniques use adaptive optics concepts for correcting aberration in images due to air turbulence. Due to mirror surface error, a reference beam can be distorted and this error is measured by a wavefront sensor. A control system is used to provide input to the actuators based on the wavefront errors. This paper discusses the control techniques and experimental results for mirror surface control. This technology has great potential for reducing mission risk and cost for space telescopes with large mirrors.

I. INTRODUCTION

For future imaging spacecraft to provide higher resolution imaging capability, larger mirrors will be required. Because of the weight and launch constraints for space-based optics systems, the mirrors will have to be segmented and light-weight, resulting in increased flexibility and lower structural frequencies. Consequently, achieving surface accuracy requirements in nanometer range for high resolution imaging with large aperture light weight mirrors becomes a challenging task.

Development of space telescopes, such as Hubble Space Telescope (HST) and James Webb Telescope, has been very challenging in terms of cost, schedule, and performance. Initial, poor wavefront quality for HST was corrected by enormously costly in-orbit astronaut servicing. There are other space telescopes that could not be repaired, such as the Deep Impact Mission which was severely defocused after launch. Considering the past experiences of major cost overrun, schedule delays and performance problems in orbit, there is great concern in starting a new program for space telescopes with large apertures.

Active surface control in orbit by using smart structures technology has the potential to reduce cost and schedule for future space telescopes and to provide higher confidence in meeting optical performance. Active optics will relax fabrication tolerances - allowing assembly to mechanical tolerance instead of optical tolerances - and result in significant reduction in time and cost for testing. Active optics can also compensate for the effects of gravity and thermal distortions in orbit.

The Actuated Hybrid Mirrors (AHMs) [1] under development by Lawrence Livermore National Laboratory, Jet Propulsion Laboratory and Northrop Grumman Xinetics is such a system. It is a hybrid structure integrating a precision Nanolaminate foil facesheet and Silicon Carbide (SiC) substrate embedded with electroactive ceramic actuators. Wavefront sensors are used to determine wavefront errors created by mirror surface errors. A control system is used to determine voltage for actuators based on the wavefront errors. The concept is similar to adaptive optics.

The Spacecraft Research and Design Center at the Naval Postgraduate School has an active research program in adaptive optics and controls for active surface space mirrors. This paper presents an overview of adaptive optics, the NPS Adaptive Optics Testbed, and control techniques for active surface mirrors.

II. ADAPTIVE OPTICS

A typical adaptive optics system used in ground telescopes to correct image aberration due to atmospheric turbulence is shown in Fig. 1. The object beam, shown in red, from a planet is distorted by atmospheric turbulence. A reference beam, in blue, which is generated by a star or artificial star passes through the same atmosphere and is distorted by the same amount. The adaptive optics system consists of a wavefront sensor that measures the reference beam phase error and uses a control system to provide input to actuators on a deformable mirror to correct the reference beam phase errors. Generally, integral control is used. Now, when the object beam passes through the deformable mirror, the image aberration due to atmosphere is corrected and the science camera will measure the aberration free image of the planet. In our application, AHM acts as a deformable mirror. More details on the deformable mirrors and

Report Documentation Page

Form Approved
OMB No. 0704-0188

Public reporting burden for the collection of information is estimated to average 1 hour per response, including the time for reviewing instructions, searching existing data sources, gathering and maintaining the data needed, and completing and reviewing the collection of information. Send comments regarding this burden estimate or any other aspect of this collection of information, including suggestions for reducing this burden, to Washington Headquarters Services, Directorate for Information Operations and Reports, 1215 Jefferson Davis Highway, Suite 1204, Arlington VA 22202-4302. Respondents should be aware that notwithstanding any other provision of law, no person shall be subject to a penalty for failing to comply with a collection of information if it does not display a currently valid OMB control number.

1. REPORT DATE OCT 2010		2. REPORT TYPE		3. DATES COVERED 00-00-2010 to 00-00-2010	
4. TITLE AND SUBTITLE Surface Control of Actuated Hybrid Space Mirrors				5a. CONTRACT NUMBER	
				5b. GRANT NUMBER	
				5c. PROGRAM ELEMENT NUMBER	
6. AUTHOR(S)				5d. PROJECT NUMBER	
				5e. TASK NUMBER	
				5f. WORK UNIT NUMBER	
7. PERFORMING ORGANIZATION NAME(S) AND ADDRESS(ES) Naval Postgraduate School, Monterey, CA, 93943				8. PERFORMING ORGANIZATION REPORT NUMBER	
9. SPONSORING/MONITORING AGENCY NAME(S) AND ADDRESS(ES)				10. SPONSOR/MONITOR'S ACRONYM(S)	
				11. SPONSOR/MONITOR'S REPORT NUMBER(S)	
12. DISTRIBUTION/AVAILABILITY STATEMENT Approved for public release; distribution unlimited					
13. SUPPLEMENTARY NOTES 61th International Astronautical Congress, Prague, Czech, September 27-October 1, 2010					
14. ABSTRACT					
15. SUBJECT TERMS					
16. SECURITY CLASSIFICATION OF:			17. LIMITATION OF ABSTRACT	18. NUMBER OF PAGES	19a. NAME OF RESPONSIBLE PERSON
a. REPORT	b. ABSTRACT	c. THIS PAGE			
unclassified	unclassified	unclassified	Same as Report (SAR)	7	

wavefront sensors at NPS are given in the following sections.

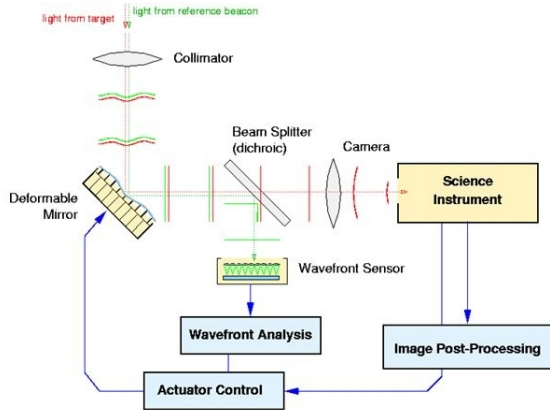


Fig. 1: Adaptive Optics System

Deformable Mirrors

Two OKO Technologies deformable mirrors are used in the experimental setup, a Mirror Membrane Deformable Mirror and a Piezo-electric Deformable Mirror. The MMDM is a membrane mirror, with a 5 μm membrane mounted over a two dimensional array of electrodes as shown in Fig 2.

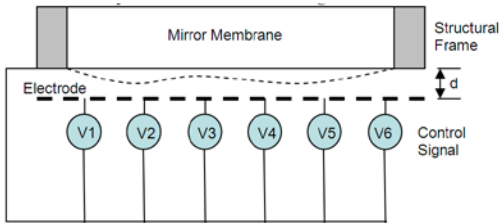


Fig. 2: Mirror Membrane Deformable Mirror

By applying a potential between the electrodes and the membrane, the membrane shape deforms. It has 37 channels (one for each actuator) with 15 mm diameter mirror surface. This mirror is built by OKO Technologies.

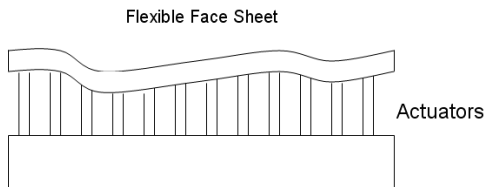


Fig. 3: Simplified Piezo-electric Deformable Mirror Schematic

The Piezo-electric Deformable Mirror (PDM), shown in Fig. 3, is made from a thin solid plate of glass. The plate is bonded to a two dimensional array of piezoelectric actuators. By elongating the piezoelectric

actuators, the mirror deforms. The current PDM in the testbed is also built by OKO and has 19 channels and a 30 mm diameter.

Shack-Hartmann Wavefront Sensors

Two wavefront sensors installed on the Adaptive Optics Testbed provide separate closed loop control of the two deformable mirrors. Both wavefront sensors are Shack-Hartmann and built by OKO Technologies. Each Shack-Hartmann wavefront sensor has 127 lenslet elements. The principle of the Shack-Hartmann wavefront sensor is shown through geometry in Figure 4. The Shack-Hartmann wavefront sensor consists of a lenslet array in front of a CMOS sensor. Each hole on the lenslet array acts as an aperture, and since the source light passing through each lenslet is converging, the image produced on the sensor is an array of spots. The position of the spots in the array is directly proportional to the local wavefront slope at each lenslet. The geometry of the 127 lenslet array used in the testbed is shown in Fig 5.

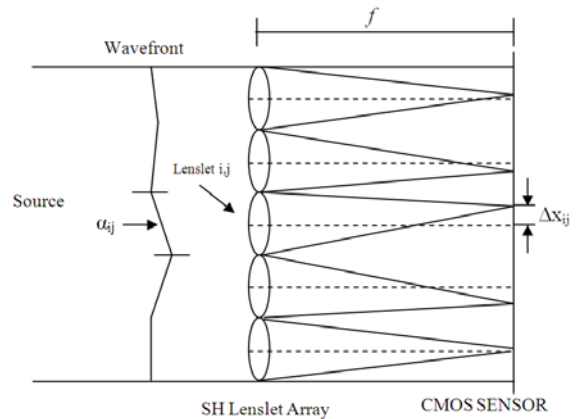


Fig. 4: Shark-Hartmann wavefront sensor principles

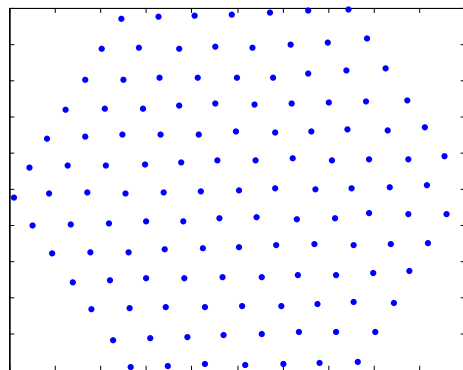


Fig. 5: Shark-Hartmann Sensor Lenslet Points

The local wavefront slopes denoted by α_{ij} and β_{ij} for the x and y directions respectively can be determined

by the Shack-Hartmann measurements corresponding to the lateral shifts, Δx_{ij} and Δy_{ij} (Fig 4), of the local focal point on the sensor. Equation (7) and (8) describes this relationship where λ is the wavelength of the reference light source and f is the focal length of the lenses in the lenslet array.

$$\alpha_{ij} = \frac{2\pi}{\lambda f} \Delta x_{ij}, \quad \beta_{ij} = \frac{2\pi}{\lambda f} \Delta y_{ij} \quad (1)$$

III. ADAPTIVE OPTICS CONTROL TESTBED

The Adaptive Optics Testbed was constructed to test adaptive optics control techniques for surface control of flexible space mirrors. A picture of the testbed is shown in Fig 6 and a schematic is shown in Fig 7.

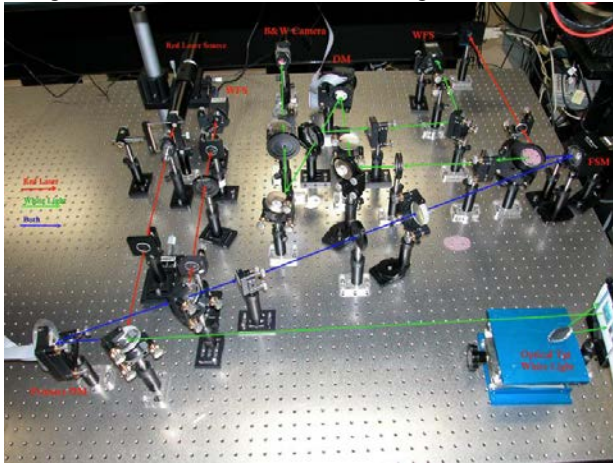


Fig. 6: Adaptive optics testbed

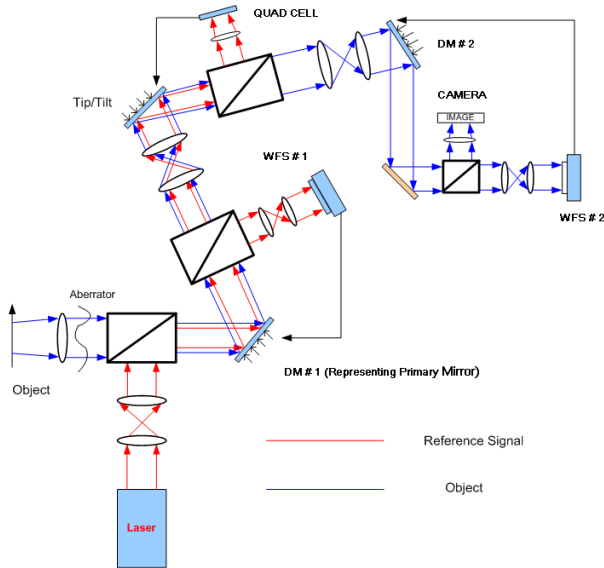


Fig. 7: Schematic of adaptive optics control testbed

In the testbed, the AHM is represented by a Mirror Membrane Deformable Mirror (DM #1 in Fig 7). The reference beam shown in red in Fig 7 is generated on the spacecraft and is used to measure the aberration caused by the primary mirror and the beam jitter onboard the spacecraft. The object beam shown in blue. Interference filters and beam splitters are used to isolate the reference beam to measure aberrations caused by the primary mirror surface and jitter.

There are three different control loops present, the first of which deals with aberrations in the primary mirror. The primary mirror onboard a spacecraft (AHM, DM #1) will be subjected to some errors created by bias voltages to the actuators. This deformation will be corrected using a Shack Hartmann wavefront sensor and the actuators on the primary mirror. The next loop removes the jitter onboard the spacecraft. The jitter is measured using the reference beam and a position sensing detector (Quad Cell) and corrected by a fast steering mirror. The final adaptive optics loop corrects any remaining aberrations left in the beam by adaptive optics. It consists of a Piezo-electric deformable mirror and Shack-Hartmann wavefront sensor. These aberrations may be from external or internal sources. The primary mirror actuators will operate at a low frequency because of the large throw required. This means the high frequency disturbances will not be corrected by the actuators on the primary mirror but will be corrected by the second deformable mirror which operates at a higher frequency. The image can be viewed on a monitor while the aberrations are being corrected. Two lenses are used to relay the pupil from the primary mirror to the wavefront sensors to optimize measurement of the aberrations. Similar pairs of doublets are used throughout the testbed to relay the pupil to the various mirrors and sensors used. The control system is shown in Fig. 8.

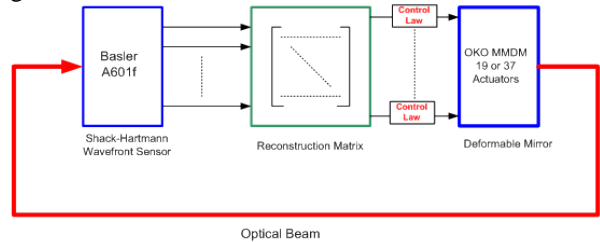


Fig. 8: Adaptive Optics Control Diagram

For a control algorithm, the adaptive optics plant is simply modeled as a static relation between input and output,

$$\mathbf{y} = \Phi \mathbf{u} \quad (2)$$

where \mathbf{y} is the sensor output, \mathbf{u} is the control input, and Φ is called the influence matrix or poke matrix. For

this simple plant, the integral controller in discrete time becomes

$$\mathbf{u}(k) = \Phi^\dagger (\mathbf{y}(k) - \mathbf{y}(k-1)) - \mu \mathbf{u}(k-1) \quad (3)$$

where Φ^\dagger represents the pseudo-inverse of the poke matrix also known as the reconstruction matrix, and μ is the adaptation gain. When the number of sensor measurements is larger than the number of inputs, the pseudo-inverse provides the least squares solution of the control input required to correct the aberration. This simple integral controller ignores the structural dynamics of a system. For a system using deformable mirror this assumption is fine as long as the fundamental natural frequencies of the deformable mirrors are around 1 KHz. However, for space telescopes with fundamental natural frequencies much lower, the control design has to take into account structures and controls interaction.

In the system, flexible dynamics were simulated by injecting a sinusoidal disturbance into the input signal. Second order discrete-time notch filters are considered in the controller which is written as

$$H_z(z) = \frac{1}{2} \left[1 + \frac{k_2 + k_1(1+k_2)z^{-1} + z^{-2}}{1 + k_1(1+k_2)z^{-1} + k_2z^{-2}} \right] \quad (4)$$

where $k_1 = -\cos(\omega_n)$, $k_2 = \frac{1 - \tan\left(\frac{BW}{2}\right)}{1 + \tan\left(\frac{BW}{2}\right)}$.

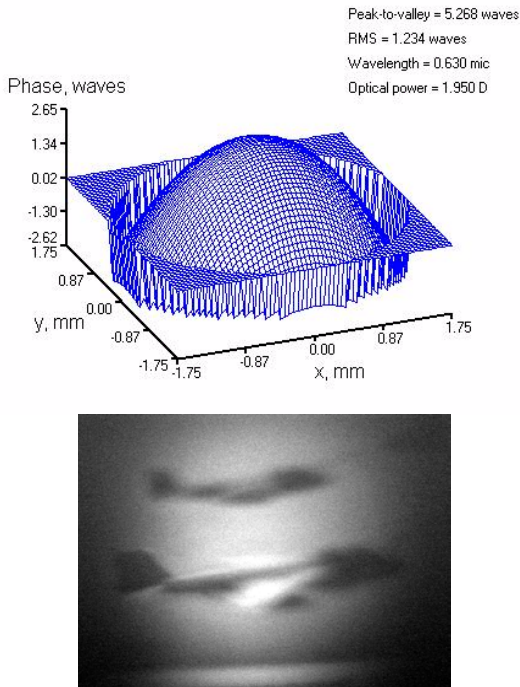


Fig. 9: Wavefront and Corresponding Image without Adaptive Optics Control

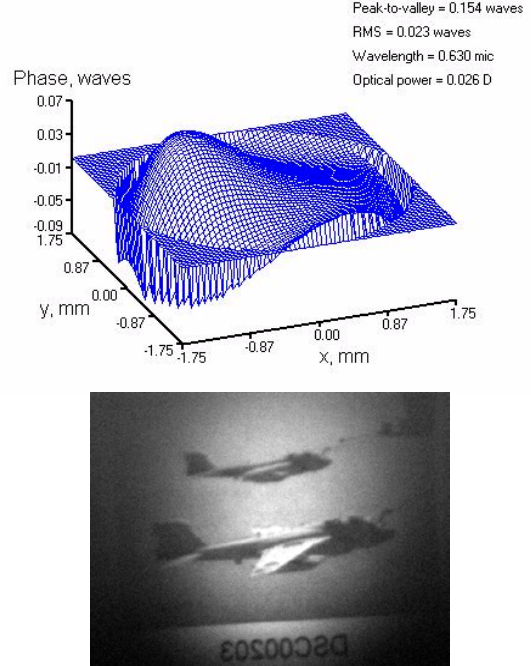


Fig. 10: Wavefront and Corresponding Image with Adaptive Optics Control

From the experiments, the wavefront error and corresponding image without adaptive optics control is given in Fig. 9. It is seen that wavefront error is 5.268 waves peak to valley and 1.234 wave RMS.

Wave front error and image with adaptive optics are shown in Fig. 10. It is shown that adaptive optics control is very effective. The wavefront error is reduced to 0.154 wave for peak to valley and 0.023 wave for RMS, which is within the diffraction limit. The corresponding image also becomes much clearer than the image without adaptive optics.

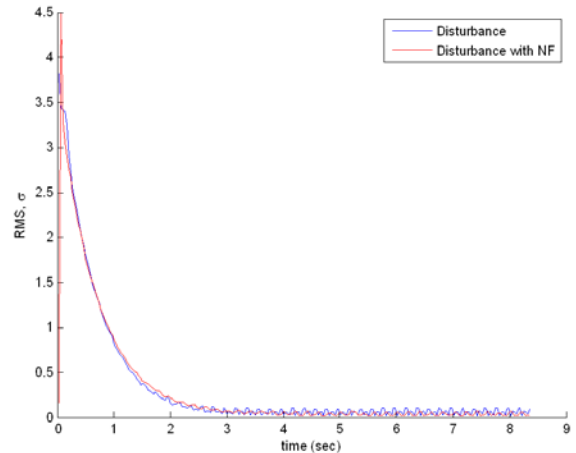


Fig. 11: Error history for 5 Hz Sinusoidal Disturbance. Amplitude of 54 Volts sinusoidal signal is added on Actuator 10 [2]

Figure 11 shows the experimental results for RMS wave front error with 5 Hz disturbance with integral control with integral and notch filter. It is shown that with a notch filter, sinusoidal wavefront error at 5 Hz is reduced.

IV. ACTUATED HYBRID MIRRORS

Actuated hybrid mirrors are hybrid structures. They integrate precision Nanolaminate foil facesheet with Silicon Carbide (SiC) substrate equipped with embedded electroactive ceramic actuators. Nanolaminate foils consist of many layers; a carbon separation layer to remove from mandrel, a layer that will form the outer surface of the mirror, such as gold for optical properties and then alternating layers of a crystalline metallic, and an amorphous layer. Nanolaminates are deposited on super polished glass or metal mandrels, which are figured to closely match the reverse of the desired optical figure. The SiC substrate is designed for lightweight, toughness, and smooth actuation. Embedded in the substrates are electrostrictive ceramic actuators that are oriented parallel to the surface of the mirror. These actuators are very low hysteresis and low creep devices. They provide both local and global influence for shape control. A reference beam is used to determine the mirror surface error by measuring the aberration of the beam by a wavefront sensor. Shack Hartman sensor that measures the slope of the wavefront phase is commonly used. A control system is used to calculate the input for the AHM actuators. In adaptive optics, integral control is used and the flexibility of the deformable mirror is neglected as the fundamental frequencies of the deformable mirrors are around 1 KHz.

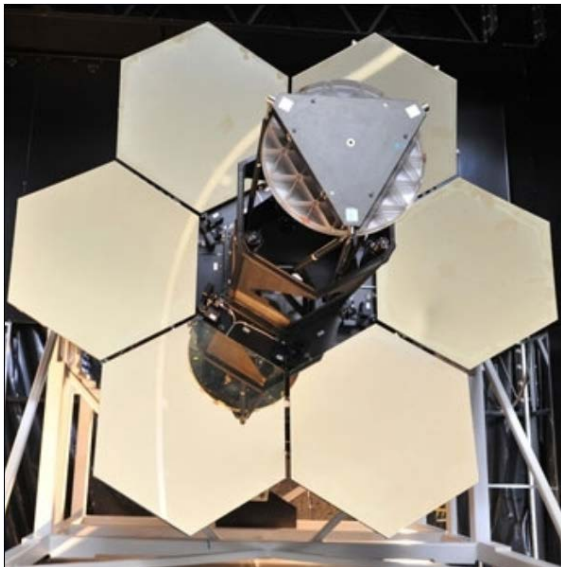


Fig. 12: Segmented Mirror Telescope

For space telescopes with large mirrors and AHM technology, the fundamental frequencies are low (~30Hz). With control bandwidth around 10-15Hz, the control system has to be designed to avoid structures and control interaction. Therefore, notch filters are added to the integral control at the critical structures frequencies. Since there are hundreds of sensor output and hundreds of actuator inputs, it is a multi-input and multi-output control problem. Modern robust control techniques, such as H-infinity, can improve the performance of the mirror.

As an example, a six-segment space telescope testbed is shown in Fig.12. It uses AHM technology. An analytical model has been developed for the system.

A state space model of the space telescope is in the following

$$\begin{aligned} \dot{x} &= Ax + Bu \\ y &= Cx + Du \end{aligned} \quad (5)$$

where x is the state variable representing 166 structural modal coordinates, y is the 936 measured output from Shack Hartman, and u is the 936 control inputs to the actuators. The matrix C represents the relationship between structural modes and wave front phase error slopes. In the frequency domain, the output of the system is

$$Y(s) = [C(sI - A)^{-1}B + D]U \quad (6)$$

When the dynamics of the system are ignored ($s=0$), the DC gain of the output becomes

$$Y(s) = [-CA^{-1}B + D]U \quad (7)$$

Therefore the poke matrix in Equation 3 can be written as

$$\Phi = -CA^{-1}B + D \quad (8)$$

In order to use classical integral control of Eq. 4, we have to obtain the pseudo-inverse of Φ . This matrix is very large and generally not properly conditioned. So it is a challenging task. For deformable mirrors with natural frequencies around 1 KHz, the flexibility effects can be neglected in the control design. However, with space telescope with AHM, the fundamental frequencies are low, around 29 Hz. For these systems, structural-control interaction becomes a challenging problem. Additional filters can be used to eliminate this structure-control interaction. Since the problem has over 900 inputs and outputs, it becomes a Multi-Input and Multi-Output control problem. The block diagram of this MIMO control system is shown in Figure 13.

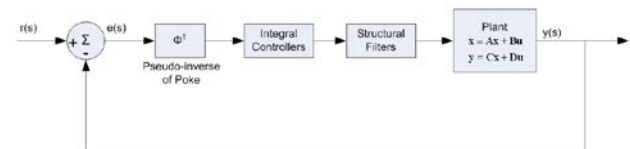
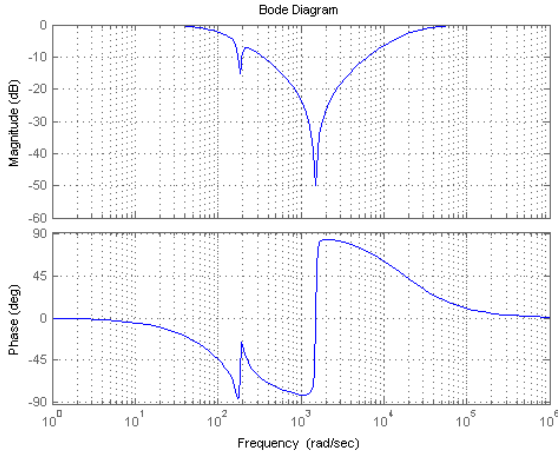
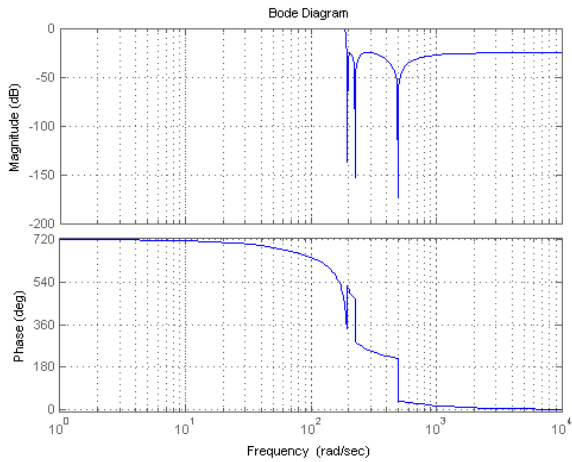


Fig. 13: Control Block Diagram of the Segmented Mirror Telescope Surface Control

The goal of the control system design is to achieve a control bandwidth of 10-15Hz. When integral controllers are used without structural filters, the bandwidth at the max gain condition was only 1.8 Hz. Any higher integral gain would make the system unstable.



(a) Notch Filter



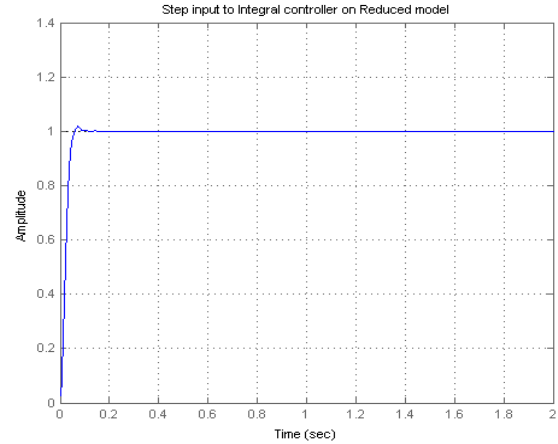
(b) Elliptical Filter

Fig. 14: Structural Filters Considered in the Control Design

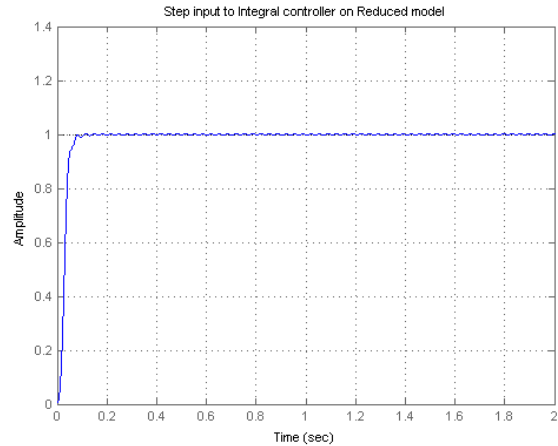
In order to reduce the structure-control interaction, a notch filter is added at 29 Hz (183 rad/sec) and 239 Hz (1500 rad/sec). These frequencies correspond to the dominant natural frequencies of the system. The bode plot of the notch filter is shown in Figure 14(a). This filter reduces the resonance peaks of dominant frequency modes, making the system stable, allowing the gain to be increased to satisfy the control bandwidth requirement of 10 Hz. Figure 15(a) shows the closed loop step response of the first sensor output when this notch filter is added to the integral control design.

The elliptic filter is another type of filter that can be used to reduce the unwanted frequency excitations. This filter has 0 dB gain at lower frequencies, and then drops off at a cutoff frequency. A sixth-order elliptic filter with

a cutoff frequency at 29 Hz (Figure 14(b)) was chosen to improve performance of the control system. The elliptic filter also helped to maintain a stable system at the required 10Hz control bandwidth. The closed loop step response for integral control with an elliptic filter is shown in Figure 15(b).



(a) Integral Control + Notch Filter



(b) Integral Control + Elliptical Filter

Fig. 15: Closed-Loop Step Response of the First Sensor Output

Further performance increase is expected when more advanced control design such as H-infinity is implemented [4]. However, overall dimensionality of the problem makes the implementation of advanced control theory and demonstration in the actual hardware extremely difficult. For future implementations of the control design, model reduction becomes crucial and several different model reduction techniques are currently being evaluated.

V. CONCLUSIONS

Active surface control of space mirrors has great potential to reduce mission risk and mission cost for space telescopes. Actuated Hybrid Mirrors have been developed to implement this technology. There are several challenges in implementing this technology. Based on the experimental results from the Adaptive Optics Testbed, adaptive optics control using integral control is quite effective in reducing wavefront to diffraction limited error. However, in this case the deformable mirror is quite rigid with fundamental structural frequency around 1 KHz. The control problem is much more complex for space mirror surface control with flexibility in the mirrors. Since the mirrors are very light and large, the natural frequencies of the mirrors are low (~30Hz) for the system. The performance requirements for surface control are stringent (nanometers). This requires the control to be of higher bandwidth. The control system has a challenging problem to avoid structural control interactions and provide high performance. The system has hundreds of sensor outputs and hundreds of actuator inputs. Therefore, it becomes a MIMO control problem. Simple addition of structural filters greatly enhances the performance of the control design. Modern control techniques such as H-infinity can be used for further performance enhancement. However, this will require model reduction to be feasible for real time control.

VI. ACKNOWLEDGEMENTS

The following Contributors have all contributed their time and effort to the results obtained on the experimental testbeds. The authors would like to sincerely acknowledge their important contributions. The contributors are Dr. Sergio Restaino, Dr. Ty Martinez, Dr. Masaki Nagashima, Capt Matt Allen, USAF, and LT Michael Looyen, USN.

REFERENCES

- [1] Hickey, G., Ealey, M., and Redding, D., "Actuated Hybrid Mirrors for Space Telescopes", SPIE Space Telescopes and Instrumentation, Vol. 7731, 773120-1, 2010.
- [2] Allen, M., Kim, J. J. and Agrawal, B., "Control of a Deformable Mirror Subject to Structural Disturbance", SPIE Defense and Security Symposium, Orland, FL, March 2008.
- [3] Zhu, L., Sun, P.C., Bartsch, D. U., Freeman, W. R., & Fainman, Y., "Adaptive Control of a Micromachined Continuous-Membrane Deformable Mirror for Aberration Compensation", Applied Optics, 38, 168-176., 1999.
- [4] Kim, J. J., Burtz, D. and Agrawal, B., "Wavefront Correction of Optical Beam for Large Space Mirrors Using Robust Control Techniques", Acta Astronautica, doi:10.1016/j.actaastro.2010.07.017, 2010.